



HAL
open science

Simulation of shock-bubbles interaction using a four-equation homogeneous model

Eric Goncalves da Silva, Dia Zeidan

► **To cite this version:**

Eric Goncalves da Silva, Dia Zeidan. Simulation of shock-bubbles interaction using a four-equation homogeneous model. International Symposium on Shock Waves, Jul 2017, Nagoya, Japan. hal-01569163

HAL Id: hal-01569163

<https://hal.science/hal-01569163>

Submitted on 26 Jul 2017

HAL is a multi-disciplinary open access archive for the deposit and dissemination of scientific research documents, whether they are published or not. The documents may come from teaching and research institutions in France or abroad, or from public or private research centers.

L'archive ouverte pluridisciplinaire **HAL**, est destinée au dépôt et à la diffusion de documents scientifiques de niveau recherche, publiés ou non, émanant des établissements d'enseignement et de recherche français ou étrangers, des laboratoires publics ou privés.

Simulation of shock-bubbles interaction using a four-equation homogeneous model

A. Eric Goncalves, B. Dia Zeidan

ENSMA, Pprime, UPR 3346 CNRS, 86962 Futuroscope Chasseneuil, France

School of Basic Sciences and Humanities, German Jordanian University, Amman, Jordan

Corresponding Author's name: eric.goncalves@ensma.fr

Abstract This paper presents a numerical study of air bubble collapse in water induced by the impact of a shock wave. Simulations are performed using an inviscid compressible one-fluid solver. Numerical results are displayed for single-bubble and twin-bubble cases in order to investigate the evolution of the maximum pressure during the collapse. The influence of the distance between bubble is also investigated.

1 Introduction

The investigation of the pressure peak developed by a collapsing cavitation bubble leading to erosion is of primary interest for hydraulic and marine applications. To clarify the physical mechanism, numerous experimental and numerical studies of the collapse of cavity in water under shock wave loading have been proposed [1, 3, 2]. Such shock-bubble interactions develop a high-speed liquid jet that penetrates through the bubble and emit a blast wave during the induced collapse. Both the jet and the shock waves are possible damaging mechanisms and worth further investigation.

In the present study, the flow field resulting from the interaction between a planar incident shock wave and one or two circular gas bubbles is investigated numerically. We describe the shock induced collapse, with particular consideration of the maximum pressure location and potential damage. Different cases are computed by varying both the distance between bubbles and the size of the second bubble. Simulations are performed using an inviscid compressible one-fluid code based on a four-equation system. It consists in solving three mixture conservation laws for the mass, momentum and energy and a transport-equation for the gas volume fraction [4, 5].

2 Models

The homogeneous mixture approach is used with the assumption of thermal and mechanical local equilibrium between pure phases. The model consists in three conservation laws for mixture quantities (mass, momentum and total energy) with an additional equation for the void ratio. The expression for the void ratio equation α is:

$$\frac{\partial \alpha}{\partial t} + \vec{V} \cdot \text{grad}(\alpha) = \left(\frac{\rho_l c_l^2 - \rho_v c_v^2}{\frac{\rho_l c_l^2}{1-\alpha} + \frac{\rho_v c_v^2}{\alpha}} \right) \text{div} \vec{V} \quad (1)$$

where c_k are the speed of sound of phase k and \vec{V} the center-of-mass mixture velocity vector. The system has a hyperbolic nature with eigenvalues: $u - c_{wallis}$, u , u , $u + c_{wallis}$ where c_{wallis} is the propagation of acoustic waves without mass transfer [8].

To close the system, an equation of state (EOS) is necessary to link the pressure and the

temperature to both the internal energy and density. For the pure phases, we used the convex stiffened gas EOS:

$$P(\rho, e) = (\gamma - 1)\rho(e - q) - \gamma P_\infty \quad \text{and} \quad T(\rho, h) = \frac{h - q}{C_p} \quad (2)$$

where $\gamma = C_p/C_v$ is the heat capacity ratio, C_p and C_v are thermal capacities, q the energy of formation of the fluid and P_∞ is a constant reference pressure. On the basis of the stiffened gas EOS for each pure phase, an expression for the pressure and the temperature can be deduced from the thermal and mechanical equilibrium assumption. It is worth noting that these expressions are available in all possible fluid states along with the function of the void ratio and mass fraction of gas $Y = \alpha\rho_v/\rho$:

$$P(\rho, e, \alpha, Y) = (\gamma(\alpha) - 1)\rho(e - q(Y)) - \gamma(\alpha)P_\infty(\alpha) \quad ; \quad T(\rho, h, Y) = \frac{h - q(Y)}{C_p(Y)} \quad (3)$$

$$\frac{1}{\gamma(\alpha) - 1} = \frac{\alpha}{\gamma_v - 1} + \frac{1 - \alpha}{\gamma_l - 1} \quad ; \quad C_p(Y) = YC_{p_v} + (1 - Y)C_{p_l}, \quad (4)$$

$$P_\infty(\alpha) = \frac{\gamma(\alpha) - 1}{\gamma(\alpha)} \left[\alpha \frac{\gamma_v P_\infty^v}{\gamma_v - 1} + (1 - \alpha) \frac{\gamma_l P_\infty^l}{\gamma_l - 1} \right] \quad ; \quad q(Y) = Yq_v + (1 - Y)q_l$$

3 Numerics

Numerical simulations are carried out using an in-house finite volume code solving the compressible inviscid system [4, 9]. Numerical fluxes are computed with a HLLC scheme. The second-order is obtained through the MUSCL extrapolation and the minmod slope limiter is used. Further, the numerical simulations of the initial-boundary value problems are accomplished using splitting approach. In such approach, one starts in solving the source-free homogeneous part of the whole system followed by solving the system of ordinary differential equations to obtain the complete solution. The numerical treatment of the boundary conditions is based on the inviscid characteristic relations.

4 Simulation results

4.1 Single-bubble case

The considered test is similar to the one presented in [1, 7]. A cylindrical air bubble, 6 mm in diameter, is immersed in a water pool, under the following initial conditions: $\vec{V} = (0, 0)$ m/s, $P = 10^5$ Pa, $\rho_{air} = 1$ kg/m³ and $\rho_{water} = 1000$ kg/m³. Due to the symmetry of the problem, we only consider a half bubble. The center of the bubble is located at (8, 0) mm in the computational domain of size 24×12 mm. The bubble is collapsed by a normal shock wave moving at $M_{sh} = 1.72$, initially located at abscissa $x_{sh} = 4$ mm. The schematic diagram of the test case is given in Figure 1. Simulations are performed using an uniform grid composed by 800×400 cells and a time step $\Delta t = 10^{-9}$ s. Parameters of the EOSs and post-shock conditions are:

$$\left(\begin{array}{c} \gamma \\ P_\infty \\ \rho \end{array} \right)_l = \left(\begin{array}{c} 4.4 \\ 6 \times 10^8 \text{ Pa} \\ 1000 \text{ kg/m}^3 \end{array} \right); \quad \left(\begin{array}{c} \gamma \\ P_\infty \\ \rho \end{array} \right)_v = \left(\begin{array}{c} 1.4 \\ 0 \text{ Pa} \\ 1 \text{ kg/m}^3 \end{array} \right); \quad \left(\begin{array}{c} P \\ \rho \\ u \end{array} \right)_{sh} = \left(\begin{array}{c} 1.9 \cdot 10^9 \text{ Pa} \\ 1323.65 \text{ kg/m}^3 \\ 681.58 \text{ m/s} \end{array} \right)$$

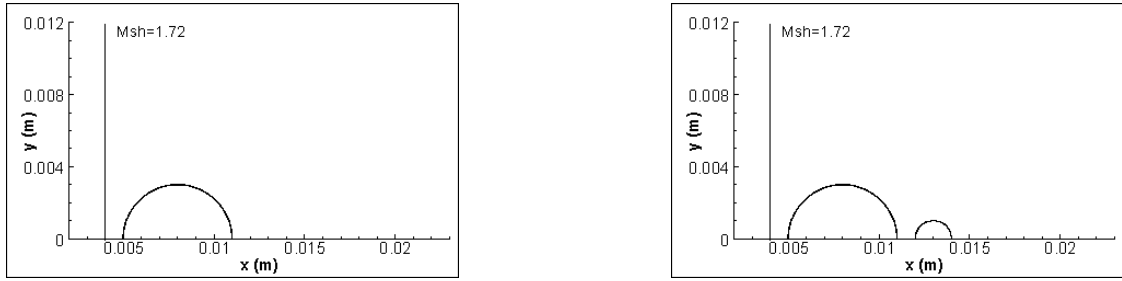


Fig.1 Initial situation for the interaction, single-bubble (left) and twin-bubble(right)

The evolution of the density gradient modulus (Schlieren-type representation) and the pressure (in bar) are plotted in Figure 2 at different instants. After the water shock wave has collided with the bubble, a strong rarefaction wave is reflected backwards from the interface, and a weak shock wave is transmitted inside of the bubble (time $t = 2\mu s$). Due to the pressure difference between both sides, the bubble is asymmetrically contracted and spreads laterally in the process. This change in shape is driven by vorticity generated at the edge of the bubble due to the passage of the wave which induces a jet of water along the axis of flow symmetry. When this water jet impacts the stationary water at the front of the bubble (at time $t=3.2 \mu s$), an intense blast wave also called water hammer shock is formed generating a high-pressure zone. The blast front, which expands continuously, is highly asymmetric due to the high-speed water jet (see Figure 2 at time $t = 3.8\mu s$). Caused by the leftward blast wave, secondary jets penetrate into the smaller bubbles and cut the initial bubble into four pieces. The interaction of the blast wave with the bubble fragments lead to high pressure levels (at time $t=4.4 \mu s$). Moreover, the low-pressure area inside the vortices core are well illustrated.

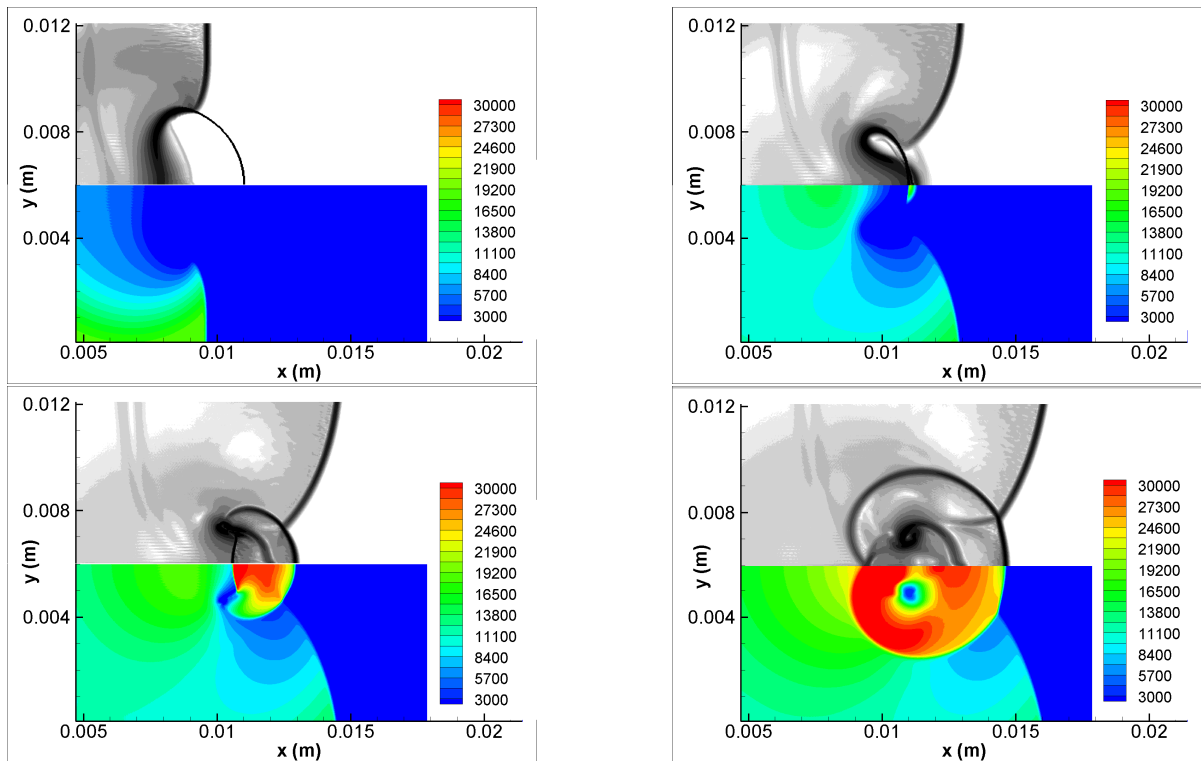


Fig.2 Evolution of the density gradient modulus and the pressure (in bar) at times $t=2, 3.2, 3.8$ and $4.4 \mu s$

The pressure evolution on the axis and the maximum pressure in the domain, plotted in Figure 3, illustrate the high pressure reached during the cavity collapse. We can observe the first peak at time $t=3.4 \mu\text{s}$ when the water jet impacts the bubble front and the second peak (more intense, around 70000 bar) at time $t=4.4 \mu\text{s}$ when the leftward blast wave collides the bubble fragments.

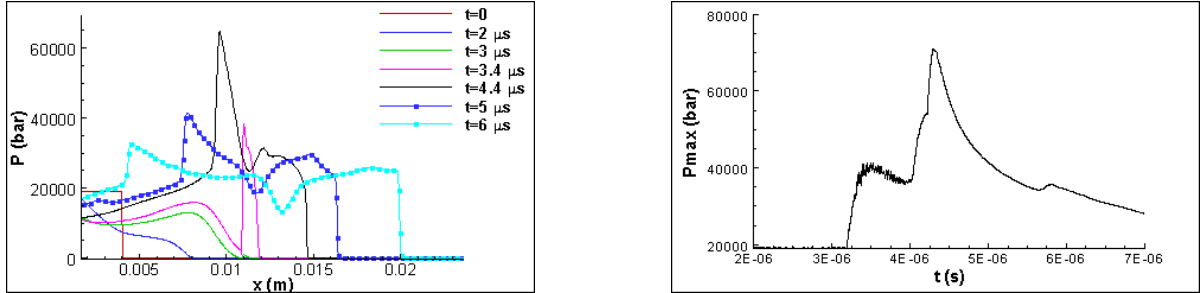


Fig.3 Evolution of the axial (left) and maximum (right) pressure during the collapse

4.2 Double-bubble case

The second test is an extension of the first one considering a second bubble placed behind the first bubble. The interdependence of bubbles and the possible intensification of the peak pressure is investigated. We introduce the distance S between the bubbles center. Different configurations are simulated by varying the inter-bubble distance and the second bubble diameter D_2 . As suggested by Betney et al. [2] for two equally sized bubbles, the peak pressure intensity relatively to the first bubble value is the most intense when the ratio S/R is smaller than 2.5. We focus in the present study on strong cases where the potential damage is high. Numerical parameters are similar to the previous case.

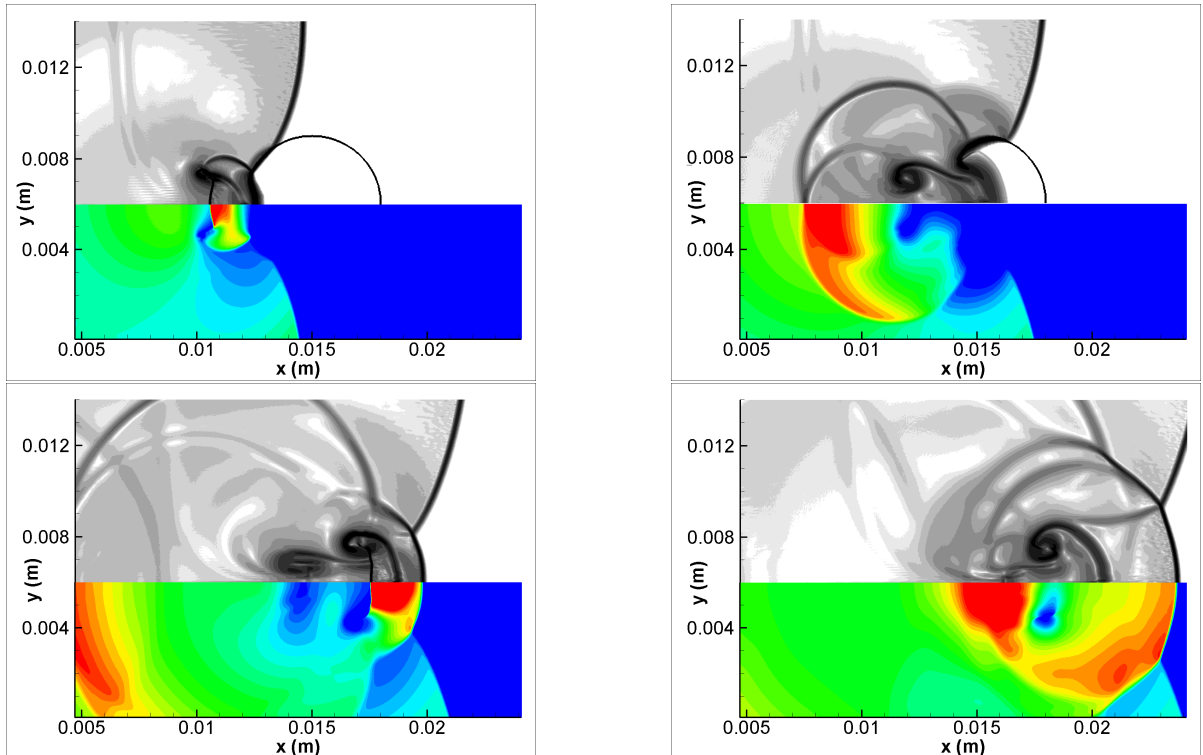


Fig.4 Schlieren and pressure visualizations at times $t=3.8, 5, 6.4$ and $7.6 \mu\text{s}$, $D_2 = D_1$

First, we consider two equally sized bubbles (diameter $D_1 = D_2 = 6$ mm) for which the distance $S = 7$ mm ($S/R = 2.33$). The evolution of the density gradient modulus and the pressure (in bar) are plotted in Figure 4. For the first bubble, the collapse is similar to the single-bubble case. As shown by Lauer et al. [6], the second bubble collapse follows the same process for which the blast wave emitted by the first collapse plays the role of the incident shock. At time $t=5 \mu\text{s}$, the transmitted shock inside the second bubble is well illustrated. When the first blast wave impacts the second bubble, a high-speed jet is formed. On impact with the right front of the second bubble, a wider blast wave is generated leading to an intense pressure peak (time $t=6.4 \mu\text{s}$). At time $t=7.6 \mu\text{s}$, the second blast wave re-collapses the first bubble fragments, leading to a very high pressure. The intensification of the second bubble collapse relative to the first one is illustrated in Figure 5 where are plotted the pressure evolution on the axis and the maximum pressure during the collapse. For the first bubble, the pressure evolution is similar to the previous case. For the second bubble, the first peak corresponding to the impact of the high-speed jet forming the second blast wave is largely more intense than the first collapse (around 50% more). The intensity of the second peak due the impact of the second blast wave with bubble pieces is similar to the first collapse pressure level.

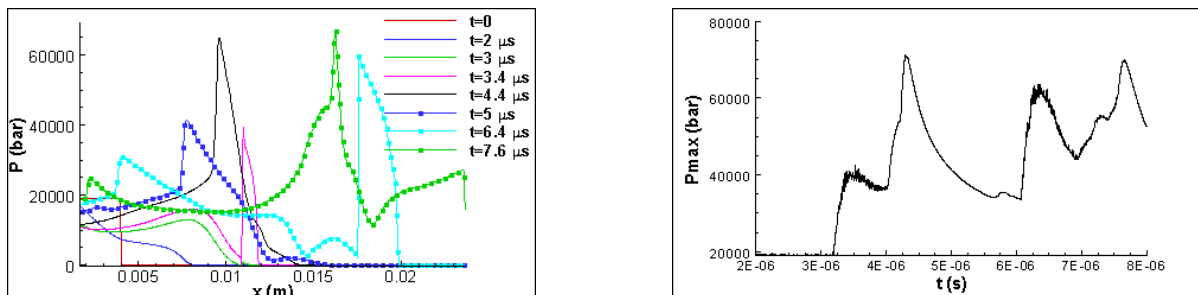


Fig.5 Evolution of the axial pressure (left) and the maximum pressure (right), $D_2 = D_1$

Secondly, we reduce the size of the second bubble for which the diameter $D_2 = D_1/3=2$ mm (see Figure 1 on the right). Different cases are simulated by varying the inter-bubble distance S from 4.5 mm to 9 mm, so S/R_1 varies from 1.5 to 3. The obtained pressure peaks are given in Table 1. For all cases, the pressure peak is more intense in comparison with the equally sized bubble case. Moreover, we observe a non-monotonic evolution of the pressure peak with the distance S . The most intense pressure peak (around 82400 bar, 15% higher than the single-bubble case) is simulated with $S=5$ mm or $S/R_1 = 1.66$.

Table 1 Maximum pressure peak (in bar) during the collapse

S/R_1	1.5	1.66	1.83	2	2.33	2.5	2.66	2.83	3
$D_2 = D_1$	-	-	-	-	70380	-	-	-	-
$D_2 = D_1/3$	73720	82380	80500	74200	76600	78140	79250	79620	77800

The pressure evolutions (maximum and axial) during the collapse are plotted in Figure 6 for cases $S/R_1=1.66$ and 2.66 , respectively. For both cases, the second bubble is collapsed by the blast wave emitted by the first bubble. For the short inter-distance, the pressure peak due to the blast wave impacting bubble pieces (at time $t=4.6 \mu\text{s}$) is the most intense phenomenon. At time $t=6 \mu\text{s}$, the blast wave impacts the first bubble fragments generating a pressure peak around 50000 Pa. For the second case, the pressure peak due to

the water jet impact on the bubble interface is around 60000 bar (50 % more intense in comparison with the first bubble). At time $t=5.8 \mu\text{s}$, the most intense peak is generating by the impact of the blast wave with bubble pieces. Another peak (around 45000 bar) appears at time $t=7.6 \mu\text{s}$ when the blast wave re-collapses the first bubble fragments.

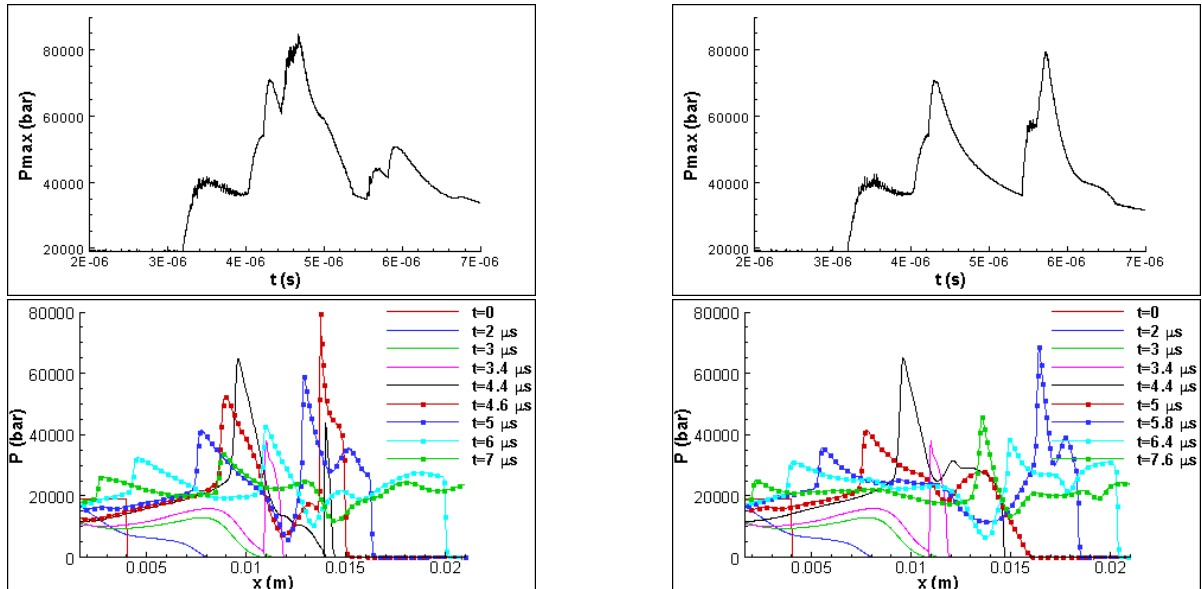


Fig.6 Evolution of axial and maximum pressure during the collapse, $S/R_1 = 1.66$ (left) and $S/R_1 = 2.66$ (right), $D_2 = D_1/3$.

5 Conclusion

This paper introduces a four-equation model for the simulation of shock-bubble interactions leading to the cavity collapse. For the single-bubble case, simulations captured the most phenomenon associated to this interaction such as the water jet formation, the bubble division, the formation of a high-pressure zone and the generation of a strong blast wave shock which expands in the liquid. Inter-bubble effects are studied through a double-bubble collapse case. It is observed that the collapse of the second bubble is preceded by the blast wave emitted by the first bubble collapse. Moreover, the second bubble collapse is even more intense than the first one leading to an amplification phenomenon. The variation of the inter-bubble distance shows that this parameter has a significant effect on the pressure peak generation.

References

- [1] G.J. Ball et al., Shock Waves **10**, 265 (2000)
- [2] M.R. Betney et al., Phys. Fluids. **27**, 036101 (2015)
- [3] N.K. Bourne, Shock Waves **11**, 447 (2002)
- [4] E. Goncalves, Computers & Fluids **72**, 1 (2013)
- [5] E. Goncalves, B. Charriere, Int. J. Multiphase Flow **59**, 54 (2014)
- [6] E. Lauer et al., Phys. Fluids. **24**, 052104 (2012)
- [7] R.R. Nourgaliev et al., J. Comput. Physics. **213**, 500 (2006)
- [8] G. Wallis, *One-dimensional two-phase flow*, (New York, McGraw-Hill, 1967)
- [9] D. Zeidan, Int. J. of Comput. Fluid Dyn. **25**, 299 (2011)